

## Accepted Manuscript

A new pyrazolone based ternary Cu(II) complex: Synthesis, characterization, crystal structure, DNA binding, protein binding and anti-cancer activity towards A549 human lung carcinoma cells with a minimum cytotoxicity to non-cancerous cells

Komal M. Vyas, R.N. Jadeja, Dipak Patel, R.V. Devkar, Vivek K. Gupta

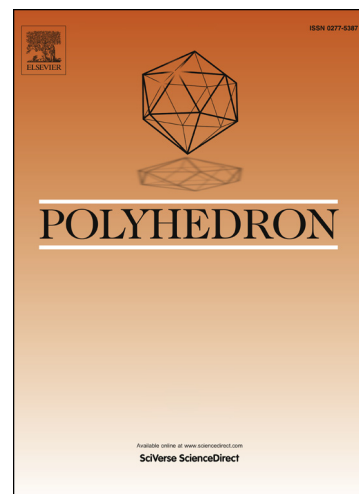
PII: S0277-5387(13)00614-1  
DOI: <http://dx.doi.org/10.1016/j.poly.2013.08.051>  
Reference: POLY 10311

To appear in: *Polyhedron*

Received Date: 20 April 2013  
Accepted Date: 6 August 2013

Please cite this article as: K.M. Vyas, R.N. Jadeja, D. Patel, R.V. Devkar, V.K. Gupta, A new pyrazolone based ternary Cu(II) complex: Synthesis, characterization, crystal structure, DNA binding, protein binding and anti-cancer activity towards A549 human lung carcinoma cells with a minimum cytotoxicity to non-cancerous cells, *Polyhedron* (2013), doi: <http://dx.doi.org/10.1016/j.poly.2013.08.051>

This is a PDF file of an unedited manuscript that has been accepted for publication. As a service to our customers we are providing this early version of the manuscript. The manuscript will undergo copyediting, typesetting, and review of the resulting proof before it is published in its final form. Please note that during the production process errors may be discovered which could affect the content, and all legal disclaimers that apply to the journal pertain.



A new pyrazolone based ternary Cu(II) complex: Synthesis, characterization, crystal structure, DNA binding, protein binding and anti-cancer activity towards A549 human lung carcinoma cells with a minimum cytotoxicity to non-cancerous cells

Komal M. Vyas<sup>a</sup>, R. N. Jadeja<sup>a\*</sup>, Dipak Patel<sup>b</sup>, R. V. Devkar<sup>b</sup>, Vivek K. Gupta<sup>c</sup>

<sup>a</sup>Department of Chemistry, Faculty of Science, The M. S. University of Baroda, Vadodara 390 002, India

<sup>b</sup>Division of Phytotherapeutics and Metabolic Endocrinology, Faculty of Science, The M.S. University of Baroda, Vadodara 390002, Gujarat, India

<sup>c</sup>Post-Graduate Department of Physics & Electronics, University of Jammu, Jammu Tawi 180 006, India

---

\*E-mail- [rajendra\\_jadeja@yahoo.com](mailto:rajendra_jadeja@yahoo.com), Tel: +91-265-2795552 ext 30

## Abstract

With the aim of exploring the anticancer properties of coordination compounds, we report for the first time the synthesis of the new ternary complex [Cu(TMCPMP-TS)(Phen)] (TMCPMP-TS; (Z)-2-((1-(3-chlorophenyl)-3-methyl-5-oxo-4,5-dihydro-1H-pyrazol-4-yl)(p-tolyl)methylene) hydrazinecarbothioamide and Phen; 1,10-phenanthroline). The complex was characterized by various techniques, including X-ray crystallography which showed that the geometry of the metal centre was between square pyramidal and trigonal bipyramidal. The interaction with calf-thymus DNA showed binding through intercalation. The protein binding ability with bovine serum albumin revealed a stronger binding of complex as compared to the free ligands. The anticancer activity of the complex was investigated by exposing it to the A549 (human lung cancer) cell line, which showed mitochondrial damage *via* an oxidative mechanism. After 24 hr treatment, the complex arrested S and G2/M phases in the cell cycle progression and induced cell death. The results envisaged herein indicate that Cu(TMCPMP-TS)(Phen) holds ample merit to develop it as a therapeutic agent against cancer.

**Keywords:** *pyrazolone based thiosemicarbazone, phenanthroline, ternary Cu(II) complex, DNA binding, Protein binding, Anti-cancer activity*

---

## 1. Introduction

One of the most rapidly developing areas of pharmaceutical research is the discovery of drugs for cancer therapy. Lung cancer has been recognized as one of the leading causes of death worldwide. The highly proliferative nature of cancer cells has undoubtedly been realized and consequently, inhibition of proliferative pathways is considered to be an effective strategy to fight cancer. Much attention has recently been paid to the discovery and development of new, more selective anticancer agents. Due to serious side effects and acquired drug resistance of anticancer drugs, there are considerable attempts being made to replace these drugs with suitable alternatives and therefore numerous transition metal complexes have been synthesized and tested for their anticancer activities.

Pyrazolone, as a prominent structural motif, is found in numerous active compounds. Pyrazolone derivatives have occupied a unique position in drug discovery due to their broad range of biological activities, such as anti-inflammatory, anti-bacterial, anti-microbial, anti-cancer, antioxidant and analgesic activities. Due to their easy preparation and rich biological activity [1-3], pyrazolone and its complexes have received considerable attention in coordination chemistry and medicinal chemistry. Schiff base ligands of pyrazolone and their metal complexes have been reported widely. Among these, thiosemicarbazone derivatives have been paid attention due to their rich biological properties [4-6]. This type of ligand has been reported widely to show photochromic properties by Dian-zeng Jia and co-workers [7-9], whereas the related complexes have not been explored that much [10-13]. Moreover, the ligands and their metal complexes possess strong biological activity, like DNA binding, DNA cleavage, anticancer, etc [14,15]. The biological activities of metal complexes differ from

those of either the free ligands or metal ions, and increased or decreased activities in relation to the non-complexed thiosemicarbazones have been reported for several transition metal complexes [12].

Among the transition metal complexes, Cu(II) complexes are considered the best alternatives to cisplatin because copper is biocompatible and exhibits many significant roles in biological systems. Several copper complexes containing pyridyl-type ligands, such as 1,10-phenanthroline [16], were screened for their anticancer activity [16-19].

Sigman and co-workers [20] have developed the first chemical nuclease, bis-(1,10-phenanthroline) Cu(I) complex. Recently, there has been a substantial increase in the design and study of DNA binding and cleavage properties of mixed ligand Cu(II) complexes [21-24] and the development of new copper-based metallodrugs.

Serum albumins, as the most abundant proteins in the circulatory system, act as a transporter and disposer of many endogenous and exogenous compounds [25]. Bovine serum albumin (BSA) is structurally homologous to human serum albumin (HSA) [26]. Studies on serum albumins can provide information on the structural features that determines the therapeutic effectiveness of drugs and standardized screens for protein binding in new drug design and for fixing dose limits [27]. Therefore, the binding of drugs to serum albumin *in vitro*, considered as a model in protein chemistry to study the binding behavior of proteins, has been an interesting research field in chemistry, life sciences and clinical medicine [28].

Because copper complexes containing either thiosemicarbazones or pyridyl-type ligands showed moderate anticancer activities [14-19], we considered that ternary complexes containing both types of ligands would be good candidates for the discovery of new novel anticancer metallodrugs. All of the above facts have stimulated our interest in the present work. Hence, this report describes the synthesis of a ternary Cu(II) complex derived from a 4-toluoyl pyrazolone based thiosemicarbazone and 1,10-phenanthroline, using a new synthetic

procedure. The crystal structure of this type of ternary complex has been reported for the first time. The DNA binding, protein binding and anticancer activity against A549 lung cancer cells of this kind of complex have been reported here for the first time here in detail.

## 2. Experimental

### 2.1. Materials

The compound 1-(3-chlorophenyl)-3-methyl-1H-pyrazol-5(4H)-one (MCPMP) was obtained from Nutan Dye Chem., Sachin, Surat, India. Dioxane was obtained from E. Merck (India) Ltd. Calcium hydroxide, copper nitrate trihydrate and 1,10-phenanthroline were obtained from LOBA Chem. Pvt. Ltd., Mumbai and used as supplied. Thiosemicarbazide was obtained from Sisco Research Lab. Pvt. Ltd., Mumbai, India. Absolute alcohol was obtained from Baroda Chem. Industry Ltd. and was used after distillation. Methanol was obtained from Spectrochem., Mumbai, India and was used after distillation. CT-DNA (Calf Thymus DNA) and BSA (Bovine Serum Albumin) were purchased from Sigma Aldrich. All the chemicals used were of AR grade. Solvents used in this study were purified following standard procedures [29]. Dulbecco's Modified Eagle Medium (DMEM), Trypsin Phosphate Versene Glucose (TPVG) solution Trypsin and methylthiazolyldiphenyl- tetrazolium bromide (MTT) were purchased from HiMedia Laboratories Pvt. Ltd. (Bombay, India). Fetal bovine serum (FBS) was purchased from Biosera (Ringmer, East Sussex UK) and dimethyl sulfoxide (DMSO) was purchased from the Sisco Research Laboratories Pvt. Ltd. (Mumbai, India). Rhodamine 123, 4',6-diamidino-2-phenylindole (DAPI) and 2',7'-dichlorofluorescein diacetate (DCFDA) were purchased from Sigma (Delhi, India).

### 2.2. Pharmacology

Human lung carcinoma (A549) cells were obtained from the National Centre for Cell Science, Pune, India and were seeded ( $1 \times 10^5$  cells/ T25 flask) and cultured in DMEM containing 10% FBS and 1% antibiotic-antimycotic solution at 37 °C in a water jacketed CO<sub>2</sub>

incubator (Thermo scientific, forma II). Cells were sub-cultured every third day by trypsinization with TPVG solution. The reagents used herein were filtered through a 0.22  $\mu$  filter (Laxbro Bio-medical Aids Pvt. Ltd) prior to their use for the experiment. A549 cells were maintained for a period of 24 h in the absence of Cu(TMCPMP)(Phen) at a cell density of  $5.0 \times 10^3$  cells/well in a 96 well plate for MTT and LDH assay and  $1 \times 10^5$  cells/well in a 6 well plate for LDH release assay, mitochondrial membrane potential assay, DCFDA and AO-EB staining, cell cycle analysis and Annexin V-PI staining assays.

### 2.3. Characterization techniques

The synthesized compounds were characterized using elemental analyses, FT-IR and UV-visible spectroscopy, molar conductance, magnetic measurement and X-ray crystallography. Elemental analyses (C, H, N) of the synthesized compounds were performed on a model 2400 Perkin-Elmer elemental analyzer. Infrared spectra ( $4000-400 \text{ cm}^{-1}$ , KBr discs) of the samples were recorded on a model RX 1 FTIR Perkin-Elmer spectrophotometer. The  $^1\text{H}$  NMR spectrum of the ligand was recorded with a Bruker AV 400 MHz spectrometer using DMSO- $d_6$  as the solvent and TMS as an internal reference. The mass spectrum of the ligand was recorded on a Trace GC ultra DSQ II. Electronic spectra (in DMF at room temperature) in the range 400-800 nm were recorded on a model Perkin Elmer Lambda 35 UV-VIS spectrophotometer. Fluorescence spectra were recorded on a model JASCO, FP-6300 fluorescence spectrophotometer. The molar conductivity of a  $10^{-3}$  M solution of the complex in DMF was measured at room temperature with a model Elico CM 180 digital direct reading deluxe digital conductivity meter. The copper content was determined by EDTA after decomposing the complex with  $\text{HNO}_3$ . Magnetic susceptibility measurement of the complex was carried out with a Gouy balance using  $[\text{HgCo}(\text{CN})_4]$  as the calibrant.

### 2.4. Synthesis

## Synthesis of 4-toluoyl pyrazolone [TMCPMP]

The toluoylation reaction of pyrazolone, MCPMP (1-(3-chlorophenyl)-3-methyl-1H-pyrazol-5(4H)-one), was carried out by following the standard method reported in our previous articles [15].

### 2.4.1. (Z)-2-((1-(3-chlorophenyl)-3-methyl-5-oxo-4,5-dihydro-1H-pyrazol-4-yl)(p-tolyl)methylene) hydrazinecarbothioamide [TMCPMP-TS]

2-(3-Chloro-phenyl)-5-methyl-4-(4-methyl-benzoyl)-2,4-dihydro-pyrazol-3-one (TMCPMP, 0.326 g, 1 mmol) and thiosemicarbazide (0.091 g, 1 mmol) in ethanol (50 mL) were refluxed for 6 h in round bottom flask. During the reflux a microcrystalline yellow compound [TMCPMP-TS] separated out, which was isolated by filtration, dried in air and finally crystallized in the appropriate solvent [15(a)].

TMCPMP-TS consists of light yellow crystals. Yield 85.33 %. M.p. 198 °C Anal. calc. for  $C_{19}H_{18}ClN_5OS$  (M.W.: 399.90): C, 57.07; H, 4.54; N, 17.51; S, 8.02; found: C, 57.01; H, 4.43; N, 17.44; S, 7.95%;  $^1H$  NMR (DMSO- $d_6$ )  $\delta$  ppm: 1.79 (s, 3H, PZ C-CH<sub>3</sub>), 2.34 (s, 3H, N-TL C-CH<sub>3</sub>), 7.68 (s, 2H, NH<sub>2</sub>), 10.19 (s, 1H, -OH), 7.20-7.36 (m, 4H, Ph), 7.43-7.55 (m, 4H, TL), 8.34 (s, 1H, N-CH), 9.83 (s, 1H, NH-tsc); IR (KBr)  $\nu$  (cm<sup>-1</sup>): 3274(b) (NH<sub>2</sub>), 3163(b) (NH-tsc), 839(m) (C=S), 1625(m) (C=N, cyclic), 1230 (C=N, azomethane), 1270(m) (PZ-C-CH<sub>3</sub>), 935(s) (N-N), 1476(m) (Ph-C-C), 2965(b) (Ph-C-H);  $^{13}C$  NMR (DMSO- $d_6$ )  $\delta$  ppm: 15.97-21.40 (methyl groups), 117.68-133.78 (substituted benzene ring); MS:  $m/z$  = 398.76 [ $C_{19}H_{18}ClN_5OS$ , MIP]<sup>+</sup>, 364 [ $C_{19}H_{18}N_5OS$ ]<sup>+</sup>, 334 [ $C_{17}H_{12}N_5OS$ ]<sup>+</sup>, 289 [ $C_{13}H_{14}N_5OS$ ]<sup>+</sup>, 261 [ $C_{11}H_{11}N_5OS$ ]<sup>+</sup>, 186 [ $C_5H_9N_5OS$ ]<sup>+</sup>, 156 [ $C_9H_5N_2O$ ]<sup>+</sup>, 214 [ $C_{12}H_{12}N_3O$ ]<sup>+</sup>, 187 [ $C_{10}H_9N_3O$ ]<sup>+</sup>, 91 [ $C_7H_7$ , Base peak]<sup>+</sup>.

### 2.4.2. Title complex [Cu(TMCPMP-TS)(Phen)]:

To a solution of  $\text{Cu}(\text{NO}_3)_2 \cdot 3\text{H}_2\text{O}$  (0.241 g, 1 mmol) in methanol (5 mL), a solution of TMCPMP-TS (0.399 g, 1 mmol) in methanol (10 mL) was added while stirring. To this, a solution of 1,10-phenanthroline (0.198 g, 1 mmol) in methanol (5 mL) was added in warm methanol (5 mL). The pH of the reaction mixture was maintained at around 7.5 by adding a 10% methanolic solution of ammonia. The resultant mixture was refluxed for 3 h. The solid green crystalline product obtained was filtered off, washed with methanol and dried. The solid product was dissolved in hot DMSO and was allowed to crystallize at RT. Green crystals of single crystal X-ray diffraction quality were obtained in 10-15 days. The synthesis of the complex can be summarized by Scheme 1.

(Scheme 1)

[Cu(TMCPMP-TS)(Phen)]: Green crystals; yield 78.88%. M.p > 250 °C. Anal. Calc. for  $\text{C}_{31}\text{H}_{24}\text{ClCuN}_7\text{OS}$  (M.W.: 641.63): C, 58.03; H, 3.77; N, 15.28; Cu, 9.90; found: C, 58.10; H, 3.76; N, 15.15; Cu, 9.78%. IR (KBr,  $\text{cm}^{-1}$ ): 3169(b) (NH-tsc), 1192 (C=N, azomethane), 938(s) (N-N), 1499(m) (Ph-C-C), 1582(s) (C=N, cyclic), 1192(m) (N-N), 3280(b) ( $\text{NH}_2$ ), 641(s) (C-S), 1614(m) (C=N, cyclic), 2919(b) (Ph-C-H), 492(s) (Cu-N), 457(s) (Cu-O), 421(s) (Cu-S);  $A_M/S \text{ m}^2\text{M}^{-1}$  (in DMF, r.t.): 18.

## 2.5. Crystallography

Crystals having good morphology were chosen for three-dimensional intensity data collection. X-ray intensity data of the compounds was collected at room temperature on a Bruker CCD area-detector diffractometer equipped with graphite monochromated  $\text{MoK}\alpha$  radiation ( $\lambda = 0.71073 \text{ \AA}$ ). The crystals used for data collection were of suitable dimensions, 0.30 x 0.20 x 0.10 mm. The unit cell parameters were determined by least-squares refinement of 16728 reflections. Multi-scan absorption corrections were applied, which also corrected Lorentz and polarization effects [30]. The structure was solved by direct methods using SHELXS97 [31]. All non-hydrogen atoms of the molecule were located in the best E-map.

Full-matrix least-squares refinement was carried out using SHELXL97 [31]. Hydrogen atoms were placed at geometrically fixed positions and allowed to ride on the corresponding non-H atoms with C-H = 0.93-0.96 Å, and  $U_{\text{iso}} = 1.5 U_{\text{eq}}$  of the attached C atom for methyl H atoms and  $1.2 U_{\text{eq}}$  for other H atoms. Atomic scattering factors were taken from the International Tables for X-ray Crystallography (1992, Vol. C, Tables 4.2.6.8 and 6.1.1.4). An ORTEP [32] view of the ligand and its complex, with the atomic labelling, are shown in Figs. S1 and 1, respectively. The packing diagram of the ligand is shown in Fig. S2. The geometries of the molecules have been calculated using the software PLATON [33] and PARST. [34] The crystallographic data for the complex and ligand are summarized in Tables 1 and S1, respectively. Important bond lengths and bond angles of the ligand are listed in Table S2.

## 2.6. DNA binding

All of the experiments involving the binding of complex with CT-DNA were carried out in double distilled water with trisodium citrate (Tris, 15 mM) and sodium chloride (150 mM) and adjusted to pH 7.05 with hydrochloric acid. A DMF solution of the complex was used throughout the study. The concentration of CT-DNA per nucleotide was estimated from its known extinction coefficient at 260 nm ( $6600 \text{ M}^{-1} \text{ cm}^{-1}$ ) [35]. Solutions of CT-DNA in tris buffer gave a ratio of UV absorbance at 260 and 280 nm ( $A_{260}/A_{280}$ ) of 1.8-1.9, indicating that the DNA was sufficiently free of protein. Absorption titration experiments were performed by maintaining a constant metal complex concentration (20  $\mu\text{M}$ ), while gradually increasing the concentration of DNA (5-100  $\mu\text{M}$ ). While measuring the absorption spectra, an equal amount of DNA was added to both the test solution and the reference solution to eliminate the absorbance of DNA itself.

The data were then fitted to eq 1 [36] to obtain the intrinsic binding constant  $K_b$ .

$$[\text{DNA}]/(\varepsilon_a - \varepsilon_f) = [\text{DNA}]/(\varepsilon_b - \varepsilon_f) + 1/K_b (\varepsilon_b - \varepsilon_f) \quad \dots (1)$$

where [DNA] is the concentration of DNA in base pairs,  $\epsilon_a$  is the extinction coefficient observed for the MLCT absorption band at the given DNA concentration,  $\epsilon_f$  is the extinction coefficient of the free complex in solution and  $\epsilon_b$  is the extinction coefficient of the complex when fully bound to DNA. A plot of  $[\text{DNA}]/[\epsilon_a - \epsilon_f]$  versus [DNA] gave a slope of  $1/[\epsilon_a - \epsilon_f]$  and Y intercept equal to  $(1/K_b)[\epsilon_b - \epsilon_f]$ . The intrinsic binding constant  $K_b$  is the ratio of the slope to the intercept [36].

Competitive studies of the compound with ethidium bromide (EB) have been investigated by fluorescence spectroscopy in order to examine whether the compound can displace EB from its CT DNA-EB complex. The CT DNA-EB complex was prepared by adding 3.3  $\mu\text{M}$  EB and 4.2  $\mu\text{M}$  CT-DNA in buffer (150 mM NaCl and 15 mM trisodium citrate at pH 7.05). The intercalating effect of the compound with the DNA-EB complex was studied by adding a certain amount of a solution of the compound step by step (0-30  $\mu\text{M}$ ) into the solution of the DNA-EB complex. The influence of the addition of each compound to the DNA-EB complex solution has been obtained by recording the variation of fluorescence emission spectra. The emission spectra were monitored by keeping the excitation of the test compound at 546 nm and the emission was monitored in the range of 550-750 nm. The emission was observed at 610 nm.

Commonly, fluorescence quenching can be described by the following Stern-Volmer equation (eq 2) [37].

$$F_0/F = 1 + K_{sv}[Q] = 1 + k_q \tau_0 [Q] \quad \dots\dots (2)$$

where  $F_0$  and  $F$  are the steady-state fluorescence intensities in the absence and presence of quencher, respectively,  $K_{sv}$  is the Stern-Volmer quenching constant, obtained from the slope of the plot of  $F_0/F$  versus [Complex],  $[Q]$  is the total concentration of

quencher,  $k_q$  is the bimolecular quenching constant and  $\tau_0$  is the average lifetime of protein in the absence of quencher, and its value is  $10^{-8}$  s.

The apparent DNA binding constant ( $K_{app}$ ) values of the complex were obtained from the fluorescence spectral measurement. The  $K_{app}$  values were obtained from the equation:

$$K_{app} \times [complex]_{50} = K_{EB} \times [EB] \quad \dots\dots (3)$$

where  $K_{app}$  is the apparent binding constant of the complex studied,  $[complex]_{50}$  is the concentration of the complex at 50% quenching of DNA-bound ethidium bromide emission intensity,  $K_{EB}$  is the binding constant of ethidium bromide ( $K_{EB} = 1.0 \times 10^7 \text{ M}^{-1}$ ), and  $[EB]$  is the concentration of ethidium bromide (3.3  $\mu\text{M}$ ) [38].

## 2.7. Tryptophan Quenching Studies

A similar experimental procedure was followed for the tryptophan quenching study as used for the DNA binding studies. Quenching of tryptophan residues of BSA was performed using the complex as a quencher. To solutions of BSA in buffer, increments of the quencher were added, and the emission signals at 343 nm (excitation wavelength at 296 nm) were recorded after each addition of the quencher [36].

The data were fitted with the Stern-Volmer eq 2. The Stern-Volmer constant was obtained from the slope of the plot of  $F_0/F$  versus  $[Compound]$ .

## 2.8. Anti-cancer study

### 2.8.1. Cell viability (MTT) assay

A549 cells ( $7 \times 10^3$  cells/well) were maintain in 96-well culture plates (Tarson India Pvt. Ltd.) for 24 h in the absence and presence of  $\text{Cu}(\text{TMCPMP})(\text{Phen})$ . At the end of the incubation period 10 $\mu\text{l}$  of 3-(4, 5-dimethylthiazol- 2-yl)-2, 5-diphenyl-tetrazolium bromide (MTT, 5 mg/ml) was added to the wells and the plates were incubated at 37 °C for 4 h. Later, culture media were discarded and the wells were washed with Phosphate Buffer Saline (Hi-

media, India, Pvt. Ltd.), followed by addition of 150  $\mu$ l of DMSO and subsequent incubation for 30 min. The absorbance was then read at 540 nm in an ELX800 Universal Microplate Reader [39].

### **2.8.2. Cellular integrity (LDH release) assay**

A549 cells were maintained in 96 well plates for 24 h as mentioned above. Later the supernatant from each well was collected and activity levels of LDH were assayed with a commercially available kit (Reckon diagnostics Ltd., Mumbai, India) using a Merck microlab L 300 semi-auto-analyzer and the percentage cytotoxicity was calculated [39].

### **2.8.3. Intracellular ROS generation (DCFDA staining)**

After 18 h of treatment with Cu(TMCPMP-TS)(Phen), cells were incubated with 7.5  $\mu$ M 2,7-dichlorodihydrofluorescein diacetate (CM-H<sub>2</sub>-DCFDA) at 37 °C for 30 min. The cells were observed with a Leica DMRB fluorescent microscope [40].

### **2.8.4. Mitochondrial Membrane Potential**

The changes in mitochondrial membrane potential were measured using the fluorescent cationic dye Rhodamine 123 (RHO 123). After 24 h treatment with Cu(TMCPMP)(Phen), the cells were incubated with 1  $\mu$ M RHO 123 for 10 min at 37 °C. The fluorescence was determined at excitation and emission wavelengths of 485 and 530 nm, respectively using a spectrofluorometer (Jasco FP-6300, Japan) and expressed as fluorescence intensity units (FIU) [41].

### **2.8.5. Nuclear morphology assay (DAPI staining)**

Cells ( $5 \times 10^4$  cells/well) were plated into a 6-well plate. After 80% confluence, the cells were treated with or without different concentrations of Cu(TMCPMP-TS)(Phen) at 37 °C for 24 h. Single-cell suspensions of treated cells were washed with PBS and fixed with 70% ethanol for 20 min at room temperature. Cells were washed again with PBS and stained with DAPI (0.6  $\mu$ g/mL in PBS) incubated for 5 min. The nuclear morphology of apoptotic

cells with condensed/fragmented nuclei was examined under a fluorescent microscope (Leica DMRB fluorescence microscope).

### **2.8.6. Assessment of apoptosis**

#### **2.8.6.1. AO/EB staining**

A549 cells ( $1 \times 10^5$  cells/well) were maintained in 6 well plates as described earlier for 24 h. At the end of the experimental period, the cells were collected using TPVG solution. One microliter of dye mixture (1 mg/ml AO and 1mg/ml EB in PBS) was mixed with 9  $\mu$ l of cell suspension ( $0.5 \times 10^6$  cells/ml) on a clean microscope slide, examined and photographed under a Leica DMRB fluorescence microscope. A minimum of 300 cells were counted in every sample to calculate the percentage cell death.

#### **2.8.6.2. Cell cycle analysis**

Cells ( $1 \times 10^6$  cells/well) were cultured as mentioned earlier for 24 h. After incubation, the cells were washed once in ice-cold PBS and subjected to cell cycle analysis [61]. Briefly,  $1 \times 10^5$  cells were fixed in 4.5 ml of 70% (v/v) cold ethanol for 30 min, centrifuged at 400 g for 5 min. The supernatant was removed and cells were washed with 5 ml of PBS. Cells were then re-suspended in 0.5 ml of PBS and 0.5 ml of DNA extraction buffer (Mix 192 ml of 0.2 M  $\text{Na}_2\text{HPO}_4$  with 8 ml of 0.1% Triton X-100 v/v) was added. The pH was adjusted to 7.8. The cells were incubated at room temperature for 5 min and then centrifuged at 400 g for 5 min. The supernatant was discarded and the cells were re-suspended in 1 ml of DNA staining solution (200 mg of PI in 10 ml of PBS + 2 mg of DNase free RNase). The cells were then incubated for at least 30 min at room temperature in the dark and the cell cycle distribution was then analyzed on a flow cytometer (BD FACS Aria III, USA) using FlowJo (Oregon, USA).

#### **2.8.6.3. FITC Annexin-V/PI Staining**

Annexin-V FITC/ Propidium iodide double staining assay was used to quantify apoptosis, according to the manufacturer's protocol (Invitrogen, UK). After incubation, the cells were harvested using TPVG solution and washed with ice-cold PBS and suspended in 100  $\mu$ l of  $1 \times$  binding buffer (10 mM HEPES, 140 mM NaCl and 2.5 mM CaCl<sub>2</sub>, pH 7.4). To this mixture, 5  $\mu$ l of annexin V-FITC conjugate and 1  $\mu$ l of propidium iodide solution were added to each cell suspension, followed by incubation for 15 min at room temperature in the dark. Later, the samples were analyzed on a flow cytometer (BD FACSAria III, USA) using FlowJo (Oregon, USA). Double staining of cells with FITC Annexin-V and PI enabled the discrimination of live cells (FITC<sup>-</sup>PI<sup>-</sup>), early apoptotic (FITC<sup>+</sup>PI<sup>-</sup>), late apoptotic (FITC<sup>+</sup>PI<sup>+</sup>) or necrotic cells (FITC<sup>-</sup>PI<sup>+</sup>).

#### **2.8.6.4. Statistical analysis**

The data were analyzed for statistical significance using one way analysis of variance (ANOVA) followed by Bonferroni's multiple comparison test and the results were expressed as mean  $\pm$  SEM using Graph Pad Prism version 3.0 for Windows, Graph Pad Software, San Diego, California, USA.

### **3. Results and discussion**

#### **3.1. Synthesis**

The present work stems from our interest in designing new symmetrical and unsymmetrical heterocyclic ligands and their mononuclear Cu(II) complexes. The ligand as well as its ternary Cu(II) complex have been synthesized in a very facile and essentially identical way. Both compounds are intensively colored, air and moisture free crystalline solids. They are soluble in common organic solvents, such as DMF, DMSO, MeCN, etc. The elemental analyses match well with the empirical formula of the ligand and the complex. The

analytical and spectroscopic data of both the compounds are presented in the experimental section.

### 3.2. Characterization

The ligand has been determined using elemental analysis, FT-IR,  $^1\text{H}$  NMR and mass spectroscopies, and by single crystal X-ray diffraction analysis, and the results are consistent with the proposed formula. The FT-IR,  $^1\text{H}$  NMR and mass spectra of the ligand are shown in Figs. S3, S4 and S5, respectively. Detailed characterization of a similar type of ligand system has been reported by us recently. However, to know the coordination behavior of the ligand, we have synthesized complexes containing this type of ligand and on the basis of this, it can act as a binegative tridentate ligand.

The ternary complex has been characterized by elemental analysis, FT-IR and UV-visible spectroscopy, molar conductance, magnetic measurements and single crystal X-ray diffraction analysis. The lesser molar conductance value of the complex in DMF ( $10^{-3}$  M solution at 25 °C) indicates that the complex is non-electrolytic in nature [42]. The elemental analyses data concur well with the planned formulae for the complex and recognize the  $[\text{Cu}(\text{TMCPMP-TS})(\text{Phen})]$  composition.

### 3.3. IR spectroscopy

On comparison of the IR spectrum of the ligand with that of the Cu(II) complex, the IR spectrum of the complex showed a major shift to lower wavenumbers by 20-30  $\text{cm}^{-1}$  for the azomethane  $\nu(\text{C-N})$  band, suggesting involvement of the azomethane-N with the Cu(II) ion in the complexation. These overall data suggest that the azomethane-N, enol-O and thiol-S groups are involved in coordination with the Cu(II) ion during complexation. In the low frequency region, the spectrum of the complex exhibits new bands which are not present in the spectrum of the ligand. These bands are at 492, 457 and 421  $\text{cm}^{-1}$  and are assigned to

$\nu(\text{Cu-N})$ ,  $\nu(\text{Cu-O})$  and  $\nu(\text{Cu-S})$ . Bands at *ca* 1,518, 1,425 and 721  $\text{cm}^{-1}$  in the mixed phen complex, assigned to  $\nu(\text{C=N})$ ,  $\nu(\text{C=C})$  and out-of-plane -CH stretching vibrations of 1,10-phenanthroline, confirm the presence of the phen ligand in the coordination sphere of the complex.

### 3.4. UV-visible spectroscopy

The visible spectrum for the complex under investigation was measured in DMF. In DMF, the complex displayed absorbance maxima in the 670–690 nm range. For five-coordinate Cu(II) complexes, this spectral feature is typical for SP or distorted SP geometries, which generally exhibit a band in the 550–660 nm range ( $d_{xz}, d_{yz} \rightarrow d_{x^2-y^2}$ ). In contrast, TBP Cu(II) complexes usually show a maximum at  $\lambda > 800$  nm ( $d_{xz}, d_{x^2-y^2} \rightarrow d_z^2$ ) with a higher energy shoulder. Thus, in DMF, the geometry about the Cu(II) centre in the complex is closer to SP. These data are consistent with the reported literature for distorted square pyramidal Cu(II) complexes [43].

### 3.5. Magnetic measurement studies

The magnetic data provide a great deal of information complementary to that available from the electronic spectrum. The room temperature magnetic moment of the complex is 1.78 BM, which is close to one electron paramagnetism of a mononuclear Cu(II) ion.

### 3.6. Crystal structure description of the title complex

The molecular structure and the atom labelling scheme is shown in Fig. 1. The crystallographic data of the complex are listed in Table 1. The main bond distances and angles are listed in Table 2. The packing diagram of the complex is shown in Fig. 2.

(Fig.1)

(Fig.2)

As shown in Fig. 1, the Cu(II) ion is pentacoordinated by three nitrogen atoms (azomethane N21 and pyridine N26, N37), one oxygen donor (enol O1) and one sulfur donor (thiol S25). The Cu-Nphen distances observed [Cu1-N26, 2.033(3) Å; Cu1-N37, 2.261(4) Å] fall within the range for Cu-Nimine distances observed for other diimine complexes already reported [44]. In the complex, the copper atom occupies a distorted square pyramidal environment (SP), where the basal plane is formed by three atoms (N21, S25, O1) supplied by the thiosemicarbazone ligand and one atom (N26) supplied by the phen ligand. The arm of the phen ligand completes the fifth coordination site, in the apical position (N37). The Cu–N/O/S distances of the basal plane are Cu(1)–O(1)=1.932(3), Cu(1)–N(21)=1.972(3), Cu(1)–S(25)=2.2624(11) and Cu(1)–N(26)=2.033(3) Å, and the Cu(1)–N(37) distance is 2.261(4) Å. The complex shows intermolecular interactions, which are highly relevant to binding studies. The geometry of N–H...N hydrogen bonds is listed in Table 3.

To obtain the quantitative degree of distortion of the copper polyhedron, the ratio between the two basal angles, defined as  $\tau = [(\theta - \varphi) / 60] \times 100$ , that represents the percentage of trigonal distortion from square pyramidal geometry [45], was used. For an ideal SP  $\tau$  is 0, while for an ideal TBP  $\tau$  is 100. Thus, for title complex (see Fig. 2 for labelling) the relevant angles,  $\theta = 172.21^\circ$  and  $\varphi = 152.38^\circ$  (Table 2) yield a  $\tau$  value of 33%, which indicates a geometry close to SP.

Complex formation can be proven also by comparing the X-ray data of the ligand and the title complex. It is clearly seen that there are some changes in the bond distances in the ligand on complexation. The changes are listed in Table 4. The N22–C23 bond was present as a single bond in the ligand, but its length decreased after complexation, indicating an increase in the double bond character in this bond. Also, C3–O3 was present as a double bond in the ligand, and its bond length increased after complexation, indicating an increased single bond character of this bond after complexation. Actually, the bond lengths of both these bonds are

between the single and double bonds, indicating the involvement of these bonds in resonance forms in the chelate ring after complexation.

### 3.7. DNA binding studies

It is a well-known fact that DNA is the primary pharmacological target of many antitumor compounds, and hence the interaction between DNA and metal complexes is of paramount importance in understanding the mechanism. Thus, the mode and propensity for binding of the complex to CT-DNA were studied with the aid of different techniques.

Monitoring the changes in the absorption spectra of metal complexes upon addition of increasing amounts of DNA is one of the most widely used methods for determining the overall binding constants. The absorption spectra of the complex in the absence and presence of CT-DNA (at a constant concentration of complex, 10  $\mu\text{M}$ ) is shown in Fig. 3. In the UV spectrum of the complex, the intense absorption band observed is attributed to the intraligand transition of the characteristic groups of the coordinated ligand. Any interaction between the complex and DNA could perturb the intraligand-centered spectral transitions, as observed in the UV spectra of a 10  $\mu\text{M}$  solution of the complex upon addition of DNA at different concentrations. In the UV region, the complex exhibited an intense absorption band at 270 nm, which was assigned to the  $\pi \rightarrow \pi^*$  transition of the aromatic chromophore. With increasing amounts of CT-DNA (5-100  $\mu\text{M}$ ), the absorption bands of complex are affected, exhibiting hyperchromism for the  $\pi \rightarrow \pi^*$  transition of the complex. The strong hyperchromic effect for the  $\pi \rightarrow \pi^*$  transition suggests that this complex possesses a high propensity for DNA binding.

(Fig.3)

The results derived from the UV titration experiments suggest that the complex can bind to CT-DNA [46]. The hyperchromism observed may be a first evidence of possible external binding to CT-DNA, while the existence of planar ligands may suggest stabilization

upon binding to DNA; in such a case, intercalation due to  $\pi \rightarrow \pi^*$  stacking interactions between the base pairs of CT-DNA may not be ruled out [47]. Nevertheless, the exact mode of binding cannot be merely proposed by UV spectroscopic titration studies. In order to compare quantitatively the binding strength of the complex with CT-DNA, the intrinsic binding constant  $K_b$  of the complex was determined by monitoring the changes in absorbance of the  $\pi \rightarrow \pi^*$  band with increasing concentrations of CT-DNA. The  $K_b$  value was found to be  $4.3 \times 10^4 \text{ M}^{-1}$ , suggesting that the complex has a strong binding affinity for calf thymus DNA.

The complex shows no fluorescence either in DMF or in the presence of DNA. So, the competitive DNA binding of the complex has been studied by monitoring changes in the emission intensity of ethidium bromide (EtBr) bound to CT-DNA as a function of added complex concentration to get final proof for the binding of the complex to DNA *via* intercalation. Though the emission intensity of EtBr in buffer medium is quenched by the solvent molecules [47], it is enhanced by its stacking interaction between adjacent DNA base pairs. When the complex was added to DNA pretreated with EtBr  $\{[\text{DNA}]/[\text{EtBr}]=1:1\}$ , the DNA-induced emission intensity of EtBr decreased (Fig. 4 (A)). Addition of a second DNA binding molecule would quench the EtBr emission by either replacing the DNA-bound EtBr (if it binds to DNA more strongly than EtBr) or accepting an excited state electron from EtBr. Because the complex has planar ligands, they efficiently compete with strong intercalators like EtBr for intercalative binding sites on DNA by replacing EtBr, which is reflected in the quenching of the emission intensity of DNA-bound EtBr. The titrations were also carried out for both the ligands (Figs. 4 (B & C)). The emission intensity was decreased in both the cases, but the effect was much lower as compared to the complex.

(Fig.4)

Quenching data were analyzed according to the following Stern-Volmer equation for the complex as well as for the ligands. The plot of  $F_0/F$  versus  $[Q]$  is shown in Fig. 5. The values of the Stern-Volmer constants were found to be  $1.3 \times 10^5 \text{ M}^{-1}$  (complex),  $0.6 \times 10^5 \text{ M}^{-1}$  (TMCPMP-TS) and  $0.8 \times 10^5 \text{ M}^{-1}$  (1,10-phenanthroline). The values are in good agreement with the constants observed for typical classical intercalators (ethidium-DNA,  $1 \times 10^7 \text{ M}^{-1}$ ). The diminution of the intrinsic binding constants could be explained by the steric constraints imposed by the ligand framework, thus encouraging a partial intercalation binding mode for the complex. Further, the apparent binding constant ( $K_{\text{app}}$ ) value was obtained for the complex and it was found to be  $1.1 \times 10^6 \text{ M}^{-1}$ .

(Fig.5)

These data suggested that the interaction of the Cu(II) complex with CT-DNA is stronger than that of the free ligand. Since these changes indicate only one kind of quenching process, it may be concluded that the compounds bind to CT-DNA *via* the same mode. Furthermore, such quenching constants and binding constants of the ligands and Cu(II) complex suggest that the interactions of all of the compounds with DNA should be intercalation [48].

### 3.8. Protein binding studies

Tryptophan emission quenching experiments were carried out using bovine serum albumin (BSA) in the presence of the complex and the ligands to investigate their interactions with proteins. Generally, the fluorescence of BSA is caused by two intrinsic characteristics of the protein, namely tryptophan and tyrosine. Changes in the emission spectra of tryptophan are common in response to protein conformational transitions, subunit associations, substrate binding or denaturation. Therefore, the intrinsic fluorescence of BSA can provide considerable information on their structure and dynamics and is often utilized in the study of protein folding and association reactions. The quenching of the emission intensity of BSA

was observed in the presence of the complex because of the possible changes in the protein secondary structure, leading to changes in the tryptophan environment of BSA [49].

The interaction of BSA with the complex and the ligands was studied by fluorescence measurement at room temperature. A solution of BSA (5  $\mu\text{M}$ ) was titrated with various concentrations of the compounds (0-20  $\mu\text{M}$ ). The effects of the complex and the ligands on the fluorescence emission spectrum of BSA are shown in Fig. 6. The addition of the above compounds to a solution of BSA resulted in a significant decrease in the fluorescence intensity of BSA at 343 nm, up to 57.37% from the initial fluorescence intensity of BSA. This result suggests a definite interaction of the compounds with the BSA protein [50].

(Fig.6)

The Stern-Volmer constants were calculated for this system and the values were found to be  $1.7 \times 10^5 \text{ M}^{-1}$  (complex),  $1 \times 10^5 \text{ M}^{-1}$  (TMCPMP-TS) and  $0.6 \times 10^5 \text{ M}^{-1}$  (1,10-phenanthroline). These constants were calculated from the slope of the plot  $F_0/F$  versus [Compound] (Fig. 7). The  $K_{sv}$  values suggest that the complex has a higher binding propensity than the ligands. The bimolecular constant  $K_q$  was also calculated for the complex and the ligands. The values are  $1.7 \times 10^{13} \text{ M}^{-1}\text{s}^{-1}$  (complex),  $1 \times 10^{13} \text{ M}^{-1}\text{s}^{-1}$  (TMCPMP-TS) and  $0.6 \times 10^{13} \text{ M}^{-1}\text{s}^{-1}$  (1,10-phenanthroline).

(Fig.7)

### 3.9. Anti-cancer studies

#### 3.9.1. Cell viability (MTT) and cellular integrity (LDH) release assay

Anticancer activity of Cu(TMCPMP-TS)(Phen) was assessed against A549 lung carcinoma cells by an MTT assay. Cu(TMCPMP-TS)(Phen) was able to inhibit the growth of A549 cells in a dose dependent manner ( $56.86 \pm 1.01\%$  and  $96.85 \pm 0.72\%$  at 0.12  $\mu\text{M}$  and 0.240  $\mu\text{M}$  respectively) (Fig. 8). The cytotoxic nature of Cu(TMCPMP-TS)(Phen) towards A549 cells was further confirmed by an LDH release assay. LDH enzyme leaches out of dead

cells and hence quantification of its content in the culture media indirectly reveals the extent of the cell damage [51,52] Maximum LDH release was recorded (0.240  $\mu$ M dose) in A549 cells, suggesting extensive damage to the cells following Cu(TMCPMP-TS)(Phen) treatment (Fig. 9).

(Fig.8)

(Fig.9)

### **3.9.2. Intracellular ROS generation (DCFDA staining)**

Intracellular ROS can trigger apoptosis *via* initiation of downstream signals in a cell cycle [53]. The dye (2,7 dichlorodihydrofluorescein - H<sub>2</sub>DCFDA) used in the present study crosses the cell membrane, wherein the intracellular H<sub>2</sub>O<sub>2</sub> converts the non-fluorescent H<sub>2</sub>DCFDA to DCF and emits green fluorescence [54,55]. In the present study, A549 cells showed green fluorescence following Cu(TMCPMP-TS)(Phen) treatment, with the most prominent fluorescence recorded at the 0.240  $\mu$ M dose (Fig. 10). These results indicate that Cu(TMCPMP-TS)(Phen) is instrumental in the generation of intracellular ROS in a dose dependent manner.

(Fig.10)

### **3.9.3. Mitochondrial membrane potential**

Another dye, RHO 123, accumulates in mitochondria and produces fluorescence. Its fluorescent intensity is directly proportional to the mitochondrial membrane potential of a cell, and hence RHO 123 is popularly used to assess the energy state of functional mitochondria [56]. Treatment of A549 cells with Cu(TMCPMP-TS)(Phen) resulted in a dose dependent decrement (244.00 $\pm$ 4.58 FIU and 69.33 $\pm$ 4.48 for 75 FIU and 0.240  $\mu$ M doses respectively) as compared to the untreated cells (475.70 $\pm$ 7.51) (Fig. 11). These results further strengthen the claim about the potency of Cu(TMCPMP-TS)(Phen) in induction of mitochondrial dysfunction of A549 cells in culture following 24 h treatment.

(Fig.11)

#### **3.9.4. Nuclear morphology assay (DAPI staining)**

DAPI binds to the AT rich regions of DNA and is used to distinguish the compact chromatin of apoptotic nuclei from that of normal cells. As shown in Fig. 12, exposure of A549 cells to the complex resulted in the appearance of a greater number of cells with condensed nuclei as compared to the control cells.

(Fig.12)

#### **3.9.5. Assessment of apoptosis**

##### **3.9.5.1. AO/EB staining**

Acridine Orange stains live cells (green) whereas ethidium bromide stains dead cells (red-to-orange), hence this method of dual staining enables the rapid and easy recognition/differentiation of live-dead cells when visualized under a fluorescence microscope [57]. The present study showed a dose dependent increment in EtBr positive cells following Cu(TMCPMP-TS)(Phen) treatment as compared to untreated cells. The highest dose of 0.240  $\mu$ M appeared to be the most potent in induction of cell death, as evidenced by a high number of EtBr positive and a much lower number of AO positive cells (Fig. 10).

##### **3.9.5.2. Cell cycle analysis**

The underlying mechanism involved in the inhibition of growth of A549 cells exposed to Cu(TMCPMP-TS)(Phen) was examined by assessment of the cell cycle; a method that is based on evaluation of cellular DNA content. The cell cycle analysis of a control group showed 93.8 % of cells in the  $G_0/G_1$  phase and 3.33 % of cells in the sub  $G_0/G_1$  phase, whereas the Cu(TMCPMP-TS)(Phen) treated group recorded 16.4 % cells in the  $G_0/G_1$  phase and 83.3 % of cells in the sub  $G_0/G_1$  phase (Fig. 13). As compared to the control group, a higher number of cells were recorded in the sub  $G_0/G_1$  phase, indicating that Cu(TMCPMP-TS)(Phen) induced death of A549 cells.

(Fig.13)

### 3.9.5.3. FITC Annexin-V/PI staining

Apoptosis is a process of cell death characterized by various morphological and biochemical alterations, leading to cell disruption and formation of apoptotic bodies [44]. One of the hallmarks of apoptosis is that membrane phospholipids, such as phosphatidylserine, rearrange from the inner to the outside surface of the plasma membrane and get exposed on the cell surface. This can be detected due to a high affinity for annexin V. A flow cytometric assay with Annexin V/PI double staining of control and Cu(TMCPMP-TS)(Phen) treated cells showed that the apoptosis rate was increased with Cu(TMCPMP)(Phen) treatment, wherein the treated cells recorded 20.2 % annexin V positive (early apoptotic) and 11.9 % PI positive cells (late apoptotic) (Fig. 14).

(Fig.14)

A similar cytotoxicity test (MTT assay) was also executed with rat cardiac myocytes (H9C2 cells), wherein the cells were cultured in the presence of Cu(TMCPMP-TS)(Phen). The rationale behind choosing H9C2 cells was to assess the possible cytotoxicity of Cu(TMCPMP-TS)(Phen) against a normal cell line as sensitive as rat cardiac myocytes. It was noted that Cu(TMCPMP-TS)(Phen) treated cells revealed no significant cell death, as evidenced by the fact that the results obtained that were comparable to those of the control (Fig. 8). The same needs further investigation to probe the underlying mechanism. However, the anticancer activity of Cu(TMCPMP-TS)(Phen) is possibly attributable to its ability to bring about conformational changes and cleavage of cellular DNA, and the ability to bind to the cellular proteins involved in inducing cancer.

## 4. Conclusion

This report describes the synthesis and characterization of a ternary Cu(II) complex, which has been derived from a pyrazolone based thiosemicarbazone and 1,10-phenanthroline.

The ligand and complex have been characterized by X-ray crystallography. The complex has a geometry in between SP and TBP, which has been explained on the basis of the trigonality index. DNA binding and protein binding studies have been investigated using CT-DNA and bovine serum albumin (BSA), respectively. The binding constants showed that the complex has a higher binding affinity than the ligand. An anticancer study also revealed a high grade of cytotoxicity and cell cycle arrest in the sub  $G_0/G_1$  phase, implying the potency of Cu(TMCPMP-TS)(Phen) as an anticancer agent against A549 cells. The results envisaged herein indicate that Cu(TMCPMP-TS)(Phen) holds ample merit to develop it as a therapeutic agent against cancer. Presently, we are focusing on understanding the type of interaction between the copper complex and DNA that is responsible for the cytotoxicity.

The presence of copper, with a daily intake not exceeding 4-7 mg, is safe and can minimize the above diseases. Therefore, it is appropriate to design anticancer drugs based on copper, which is anticipated to cause lower toxic effects. In this context, we have started to develop ternary complexes of Cu(II) that are expected to be less toxic but highly potent in smaller dosages compared to cisplatin and analogous compounds.

#### **Appendix A. Supplementary data**

CCDC 885025 and 815002 contain the supplementary crystallographic data for [Cu(TMCPMP-TS)(Phen)] and TMCPMP-TS, respectively. These data can be obtained free of charge via <http://www.ccdc.cam.ac.uk/conts/retrieving.html>, or from the Cambridge Crystallographic Data Centre, 12 Union Road, Cambridge CB2 1EZ, UK; fax: (+44) 1223-336-033; or e-mail: [deposit@ccdc.cam.ac.uk](mailto:deposit@ccdc.cam.ac.uk).

#### **Acknowledgement**

The authors are thankful to the University Grants Commission, New Delhi for financial assistance with this work in terms of a major research project to RNJ. They are also

thankful to the Head, Department of Chemistry and Department of Zoology for providing the necessary facilities required to carry out this work. The award of a University Research Fellowship to KMV is also gratefully acknowledged.

## References

- [1] X. H. Wang, D. Z. Jia, Y. J. Liang, S. L. Yan, Y. Ding, L. M. Chen, Z. Shi, M. S. Zeng, G. F. Liu, L. W. Fu, *Cancer Lett.*, 249 (2007) 256-270.
- [2] Z. Y. Yang, R. D. Yang, F. S. Li, K. B. Yu, *Polyhedron*, 19 (2000) 2599-2604.
- [3] A. Kimata, H. Nakagawa, R. Ohyama, T. Fukuuchi, S. Ohta, T. Suzuki, N. Miyata, J. *Med. Chem.*, 50 (2007) 5053-5056.
- [4] A. M. J. Ramanand, *J. Inorg. Biochem.* 65 (1997) 183-190.
- [5] P. K. Panchal, P. B. Pansuriya, M. N. Patel, *J. Enzym. Inhib. Med. Chem.*, 21(4) (2006) 453-458.
- [6] S. A. Patil, V. H. Naik, A. D. Kulkarni, U. Kamble, G. B. Bagihalli, P. S. Badami, J. *Coord. Chem.*, 63 (2010) 688-699.
- [7] G. Yong, G-f. Liu, L. Liu, D-z. Jia, *J. Mol. Struct: THEOCHEM*, 712 (2004) 223-231.
- [8] J. Wang, L. Liu, G-F. Liu, L. Zhang, D. Jia, *Struct. Chem.*, 18 (2007) 59-63.
- [9] B-H. Peng, G-F. Liu, L. Liu, D-Z. Jia, K-B. Yu, *J. Photochem. Photobio. A: Chemistry*, 171 (2005) 243-249.
- [10] T. Klimova, E. I. Klimova, M. Mertinez Garcia, J. M. Mendez Stivalet, L. R. Ramirez, J. *Organomet. Chem.*, 633 (2001) 137-142.
- [11] M. M. B. Pessoa, G. F. S. Andrade, V. R. P. Monteiro, M. L. A. Temperini, *Polyhedron*, 20 (2001) 3133-3141.
- [12] A. E. Liberta, D. X. West, *Biometals*, 5 (1992) 121-126.

- [13] (a) N. Raman, R. Jeyamurugan, B. Raj Kapoor, V. Mehesh, *Appl. Organometal. Chem.*, 23 (2009) 283-290. (b) V. M. Leovac, G. A. Bogdanović, L. S. Jovanović, L. Joksović, V. Marković, M. D. Joksović, S. M. Denčić, A. Isaković, I. Marković, F. W. Heinemann, S. Trifunović, I. Đalović, *J. Inorg. Biochem.*, 105 (2011) 1413-1421.
- [14] N. Raman, A. Selvan, P. Manisankar, *Spectrochim. Acta Part A.*, 76 (2010) 161-173.
- [15] (a) K. M. Vyas, R. G. Joshi, R. N. Jadeja, C. Ratna Prabha, V. K. Gupta, *Spectrochim. Acta Part A.*, 84 (2011) 256- 268; (b) R. N. Jadeja, K. M. Vyas, V. K. Gupta, R. G. Joshi, C. Ratna Prabha, *Polyhedron* 31 (2012) 767-778; (c) R. N. Jadeja, J. R. Shah, *Polyhedron* 26 (2007) 1677-1685.
- [16] M. Devereux, D. O. Shea, A. Kellett, M. McCann, M. Walsh, D. Egan, C. Deegan, K. Kedziora, G. Rosair, H. Muller-Bunz, *Synthesis, J. Inorg. Biochem.*, 101 (2007) 881-892.
- [17] N. J. Sanghamitra, P. Phatak, S. Das, A. G. Samuelson, K. Somasundaram, *J. Med. Chem.*, 48 (2005) 977-985.
- [18] R. M. Snyder, C. K. Mirabelli, R. K. Johnson, C. M. Sung, L. F. Faucette, F. L. McCabe, J. P. Zimmerman, M. Whiteman, J. C. Hempel, S. T. Crooke, *Cancer Res.*, 46 (1986) 5054-5060.
- [19] M. K. Adwankar, C. Wycliff, A. G. Samuelson, *Indian J. Exp. Biol.*, (1997) 810-814.
- [20] D. S. Sigman, A. Mazumder, M. D. Perrin, *Chem. Rev.*, 93 (1993) 2295-2316.
- [21] A. Barve, A. Kumbhar, M. Bhat, B. Joshi, R. Butcher, U. Sonawane, R. Joshi, *Inorg. Chem.*, 48 (2009) 9120-9132.
- [22] M. Chikira, Y. Tomizava, D. Fukita, T. Sugizaki, N. Sugawara, T. Yamazaki, A. Sasano, S. Shindo, M. Palaniandavar, W. E. Anthroline, *J. Inorg. Biochem.*, 89 (2002) 163-173.
- [23] B. Selvakumar, V. Rajendiran, P. U. Maheswari, H. S. Evans, M. Palaniandavar, *J. Inorg. Biochem.*, 100 (2006) 316-330.
- [24] P. A. N. Reddy, M. Nethaji, A. R. Chakravarty, *Eur. J. Inorg. Chem.*, (2004) 1440-1446.

- [25] D. C. Carter, J. X. Ho, *Adv. Protein Chem.*, 45 (1994) 153-176.
- [26] K. Hirayama, S. Akashi, M. Furuya, K. Fukuhara, *Biochim. Biophys. Res. Commun.*, 173 (1990) 639-646.
- [27] B. Sandhya, A. H. Hegde, S. S. Kalanur, U. Katrahalli, J. Seetharamappa, *J. Pharm. Biomed. Anal.*, 54 (2011) 1180-1186.
- [28] Y.-Z. Zhang, B. Zhou, Y.-X. Liu, C.-X. Zhou, X.-L. Ding, Y. Liu, *J. Fluoresc.*, 18 (2008) 109-118.
- [29] W. L. F. Armarego, D.D. Perrin, *Purification of Laboratory Chemicals*, fourth ed., The Bath Press, Butterworth-Heinemann Publication, 1997.
- [30] Bruker, SMART (Version 5.631), SAINT (Version 6.45) and SADABS (Version 2.05). Bruker AXS Inc., Madison, Wisconsin, USA, 2003.
- [31] G. M. Sheldrick, SHELXS97 and SHELXL97, Germany, University of Gottingen, 1997.
- [32] C. K. Johnson, ORTEP II; Report ORNL-5138, Oak Ridge National Laboratory, Oak Ridge, TN, 1976.
- [33] A. L. Spek, PLATON for Windows. September 1999 Version, University of Utrecht, Netherlands, 1999.
- [34] M. Nardelli, *J. Appl. Cryst.*, 28 (1995) 659.
- [35] M. E. Reichmann, S. A. Rice, C. A. Thomas, P. Doty, *J. Am. Chem. Soc.*, 76 (1954) 3047-3053.
- [36] S. S. Bhat, A. A. Kumbhar, H. Heptullah, A. A. Khan, V. V. Gobre, S. P. Gejji, V. G. Puranik, *Inorg. Chem.* 50 (2011) 545-558.

- [37] J. R. Lakowicz, Principles of Fluorescence Spectroscopy; 3rd ed. Springer Science, Business Media: New York, 2006.
- [38] M. Lee, A. L. Rhodes, M. D. Wyatt, S. Forrow, J. A. Hartley, *Biochemistry*, 32 (1993) 4237-4245.
- [39] M. C. Thounaojam, R. N. Jadeja, D. S. Dandekar, R. V. Devkar, A. V. Ramachandran, *Exp. Toxicol. Pathol.*, 64 (2010) 217-224.
- [40] M. C. Thounaojam, R. N. Jadeja, R. V. Devkar, A. V. Ramachandran, *Cardiovasc Toxicol.*, 11(2) (2011) 168-179.
- [41] R. N. Jadeja, M. C. Thounaojam, R. V. Devkar, A. V. Ramachandran, *Food Chem Toxicol.*, 49(6) (2011) 1195-202.
- [42] W. J. Geary, *Coord. Chem. Rev.*, 7 (1971) 81-122.
- [43] S. S. Massoud, F. A. Mautner, M. A. M. Abu-Youssef, N. M. Shuaib, *Polyhedron*, 18 (1999) 2061-2067.
- [44] L. Li, K. D. Karlin, S. E. Rokita, *J. Am. Chem. Soc.*, 127 (2) (2005) 520-523.
- [45] M. Duggan, N. Ray, B. Hathaway, G. Tomlinson, P. Brint, K. Pelin, *J. Chem. Soc., Dalton Trans.*, (1980) 1342-1348.
- [46] E. S. Koumoussi, M. Zampakou, C. P. Raptopoulou, V. Psycharis, C. M. Beavers, S. J. Teat, G. Psomas, T. C. Stamatatos, *Inorg. Chem.*, 51 (2012) 7699-7710.
- [47] D. S. Raja, N. S. P. Bhuvanesh, K. Natarajan, *Inorg. Chem.*, 50 (2011) 12852-12866.
- [48] Ye-Z. Zhang, X-P. Zhang, H.-N. Hou, J. Dai, Y. Liu, *Biol. Trace Elem. Res.*, 121 (2008) 276-287.
- [49] D. S. Raja, N. S. P. Bhuvanesh, K. Natarajan, *Eur. J. Med. Chem.*, 46 (2011) 4584-4594.
- [50] G. Travis, B-W. Vicki M. Roy, *Infect Immun.*, 67(9) (1999) 4367-4375.

- [51] M. Valodkar, R. N. Jadeja, M. C. Thounaojam, R. V. Devkar, S. Thakore, *Materials Science and Engineering*, 31 (2011) 1723-1728.
- [52] M. D. Evans, M. Dizdaroglu, M. S. Cooke, *Mutat Res.*, 567 (2004) 1-61.
- [53] D. A. Bass, J. W. Parce, L. R. DeChatelet, P. Szejda, M. C. Seeds, M. Thomas, J. *Immunol.*, 130 (1983) 1910-1917.
- [54] W. O. Carter, P. K. Narayanan, J. P. Robinson, *J. Leukoc. Biol.*, 55 (1994) 253-258.
- [55] R. C. Scaduto, L. W. Grotyohann, *Biophys J.*, 76 (1999) 469-477.
- [56] D. L. Spector, R. D. Goldman, L. A. Leinwand, *Cell: a laboratory manual: culture and biochemical analysis of cells*, Cold Spring Harbor Laboratory Press, New York, 1 (1998) 34.1-34.9.
- [57] P. V. AshaRani, G. L. Kah Mun, M. P. Hand, S. Valiyaveetil, *ACS Nano*, 3 (2009) 279-290.



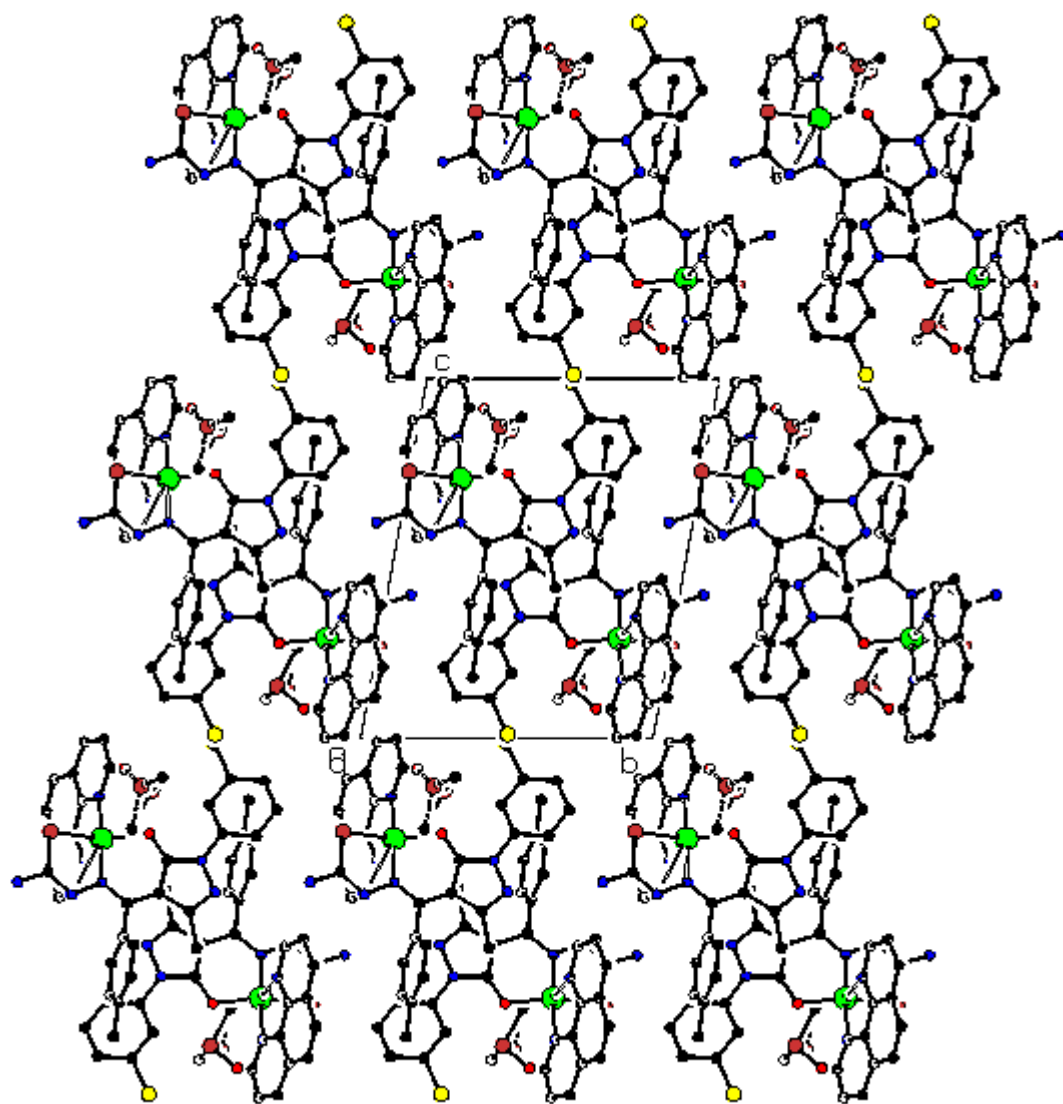


**Fig. 2.** The packing diagram of the title complex

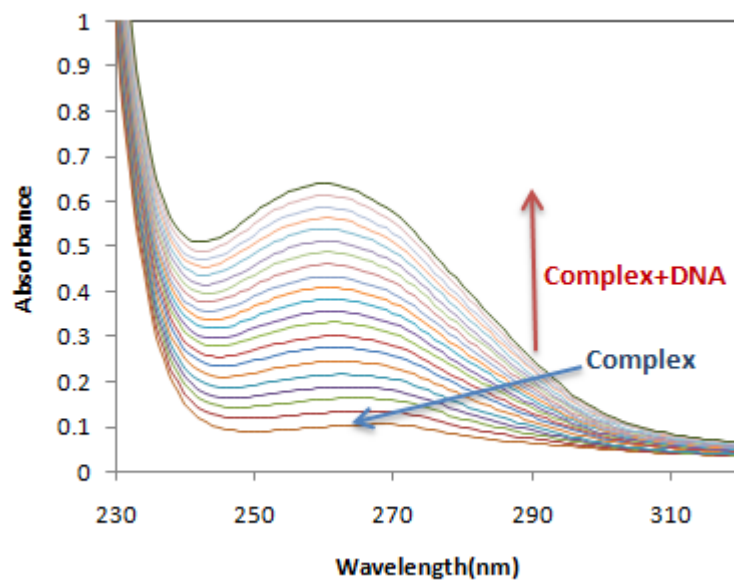


**Fig. 3.** Changes in the electronic absorption spectra of the complex (10  $\mu\text{M}$ ) with increasing concentrations (0-100  $\mu\text{M}$ ) of CT-DNA (Tris, pH 7.04). The arrow shows the changes on addition of the CT-DNA.

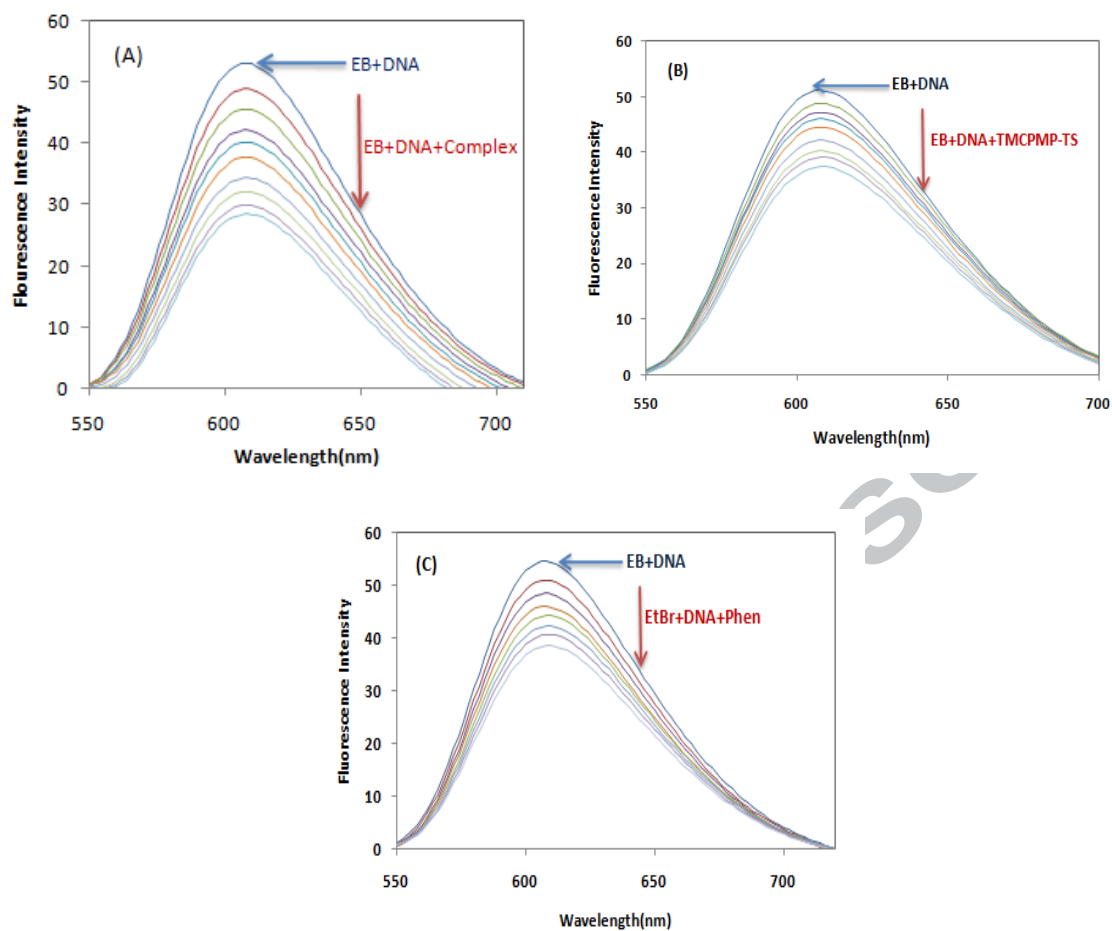


**Fig. 4.** Emission spectra ( $\lambda_{em}=610$  nm) of DNA–EB complex in buffer solution in the absence and presence of increasing amounts of (A) complex, (B) TMCPMP-TS and (C) Phen. The arrow shows the changes of intensity with increasing amounts of the compounds.

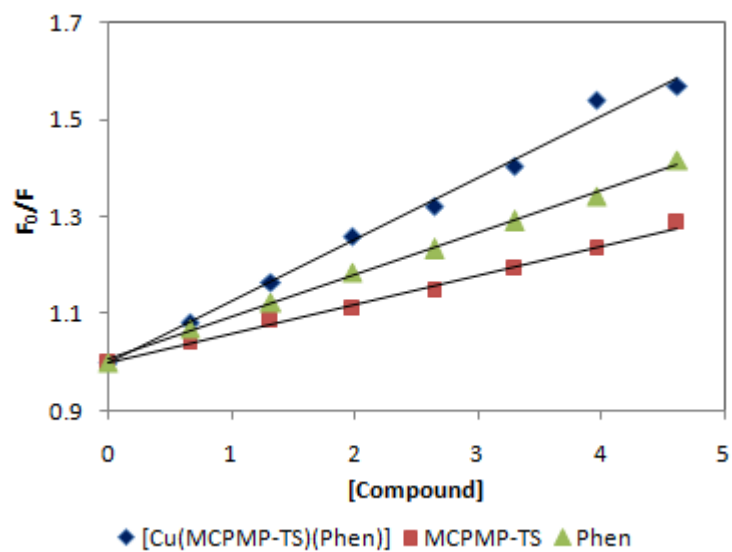


**Fig. 5.** Plot of  $F_0/F$  vs concentration for the complex and ligands in buffer solution with increasing amounts of DNA (150 mM NaCl and 15 mM trisodium citrate at pH 7.04,  $\lambda_{em} = 610$  nm).

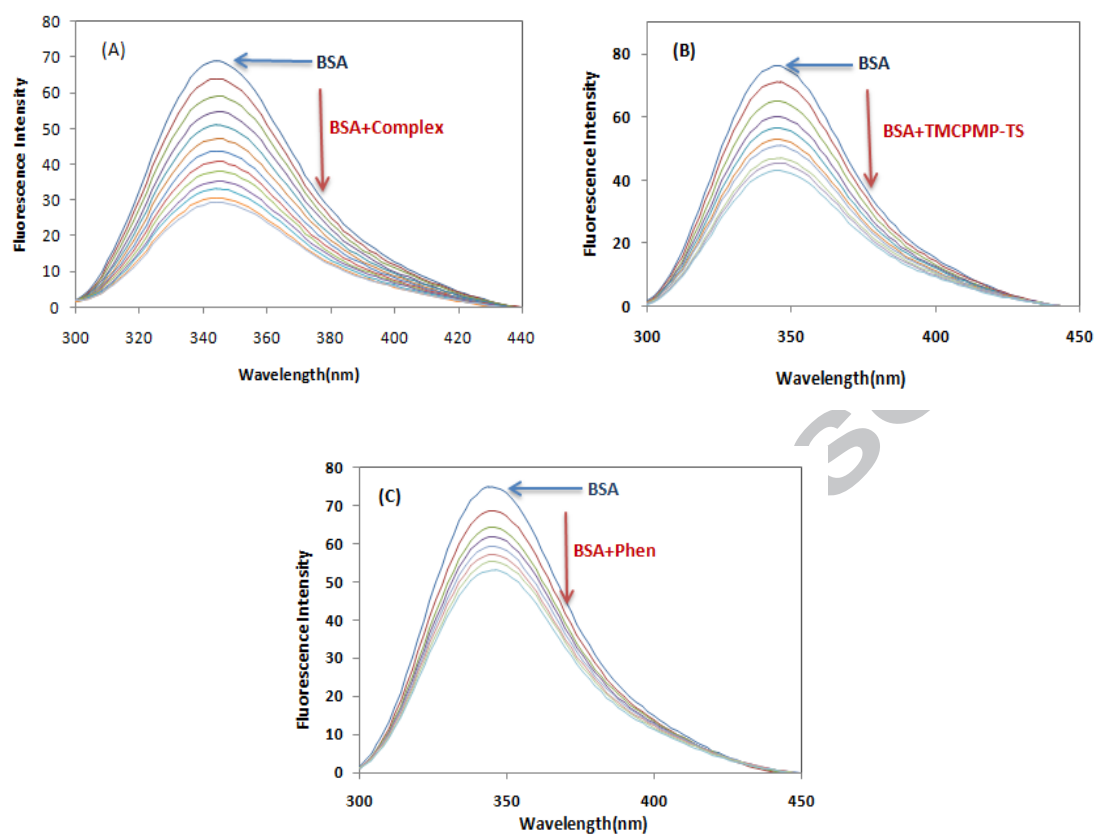


**Fig. 6.** Changes in the fluorescence spectra of BSA through its titration with (A) complex, (B) TMCMPM-TS and (C) Phen at RT. The concentration of protein is 5  $\mu\text{M}$  and the complex concentration was varied from 0-20  $\mu\text{M}$ ; pH 7.04 and  $\lambda_{\text{ex}}$  296 nm.

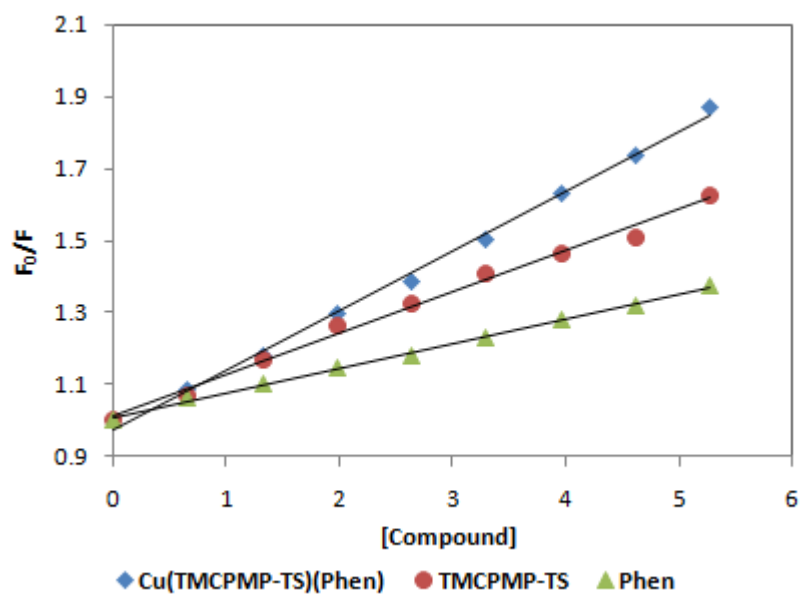


**Fig. 7.** Plot of  $F_0/F$  vs concentration of BSA in buffer solution with increasing amounts of the complex and the ligands (150 mM NaCl and 15 mM trisodium citrate at pH 7.04).

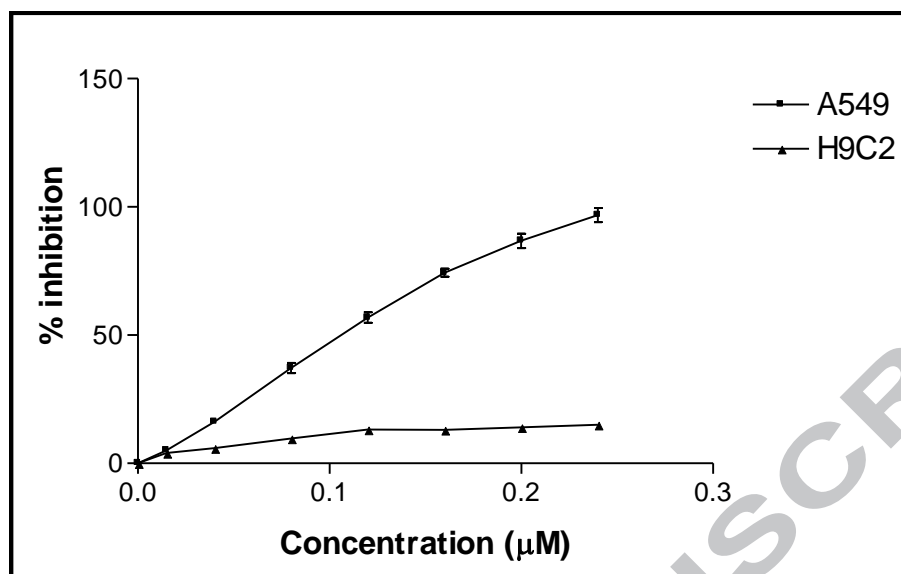


**Fig. 8.** Effect of Cu(TMCPMP-TS)(Phen) exposed to A549 cells on the cell viability.

Results are expressed as Mean  $\pm$  SEM for n = 3 (replicates)

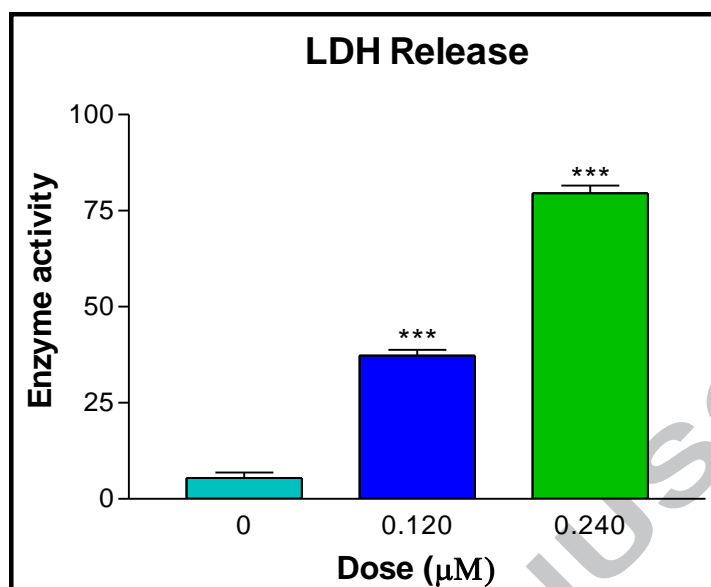


**Fig. 9.** Effect of Cu(TMCPMP-TS)(Phen) exposed to A549 cells on LDH release

Results are expressed as Mean  $\pm$  SEM for  $n = 3$  (replicates), where, ns  $p > 0.05$ , \*  $p < 0.05$ ,

\*\*  $p < 0.01$  and \*\*\*  $p < 0.001$  compared to  $0 \mu\text{M}$  [Cu(TMCPMP)(Phen)].

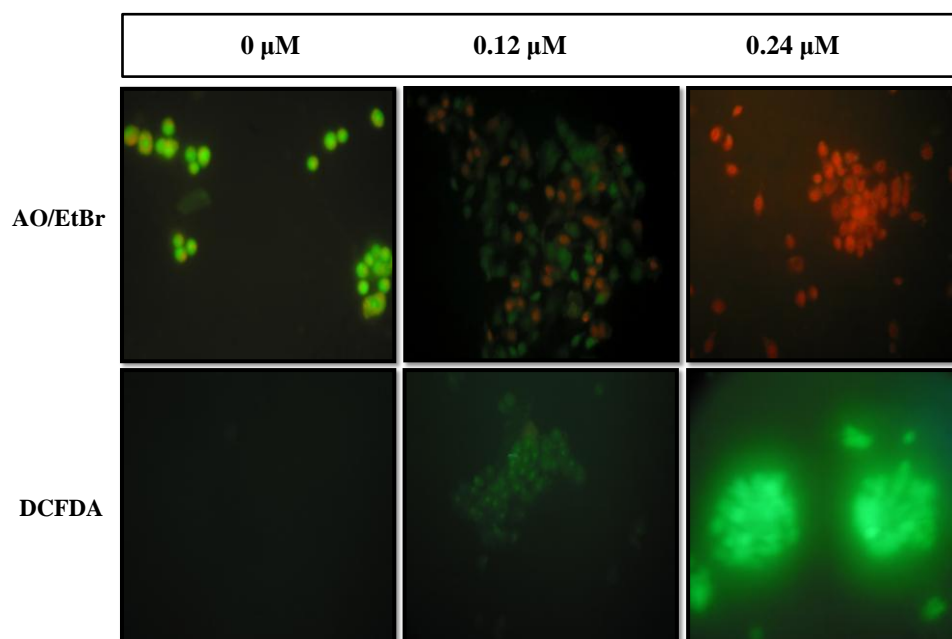


**Fig. 10.** Florescence photomicrographs of A549 cells exposed to [Cu(TMCPMP-TS)(Phen)].

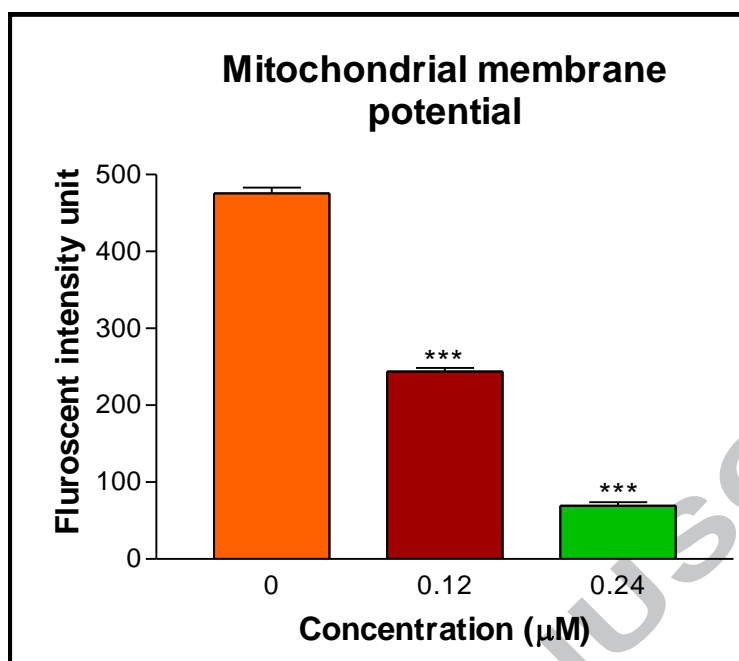


**Fig. 11.** Effect of [Cu(TMCPMP)(Phen)] exposed to A549 cells on the mitochondrial membrane potential. The results are expressed as Mean  $\pm$  SEM for  $n = 3$  (replicates), where, ns  $p > 0.05$ , \*  $p < 0.05$ , \*\*  $p < 0.01$  and \*\*\*  $p < 0.001$  compared to 0  $\mu\text{M}$  [Cu(TMCPMP-TS)(Phen)].

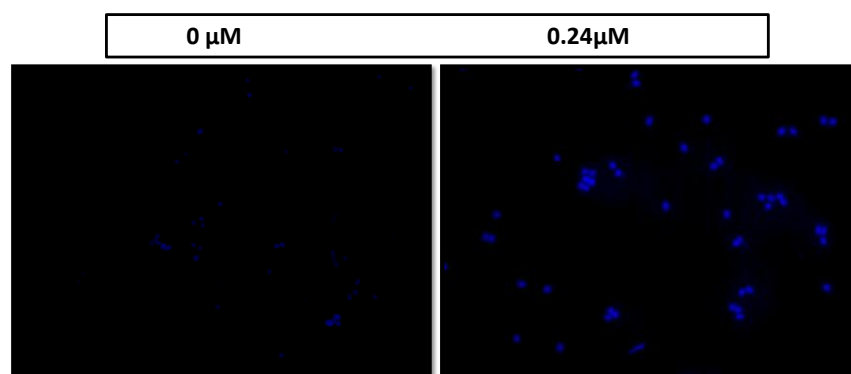


**Fig. 12.** Fluorescence photomicrographs of DAPI staining of A549 cells exposed to [Cu(TMCPMP-TS)(Phen)].

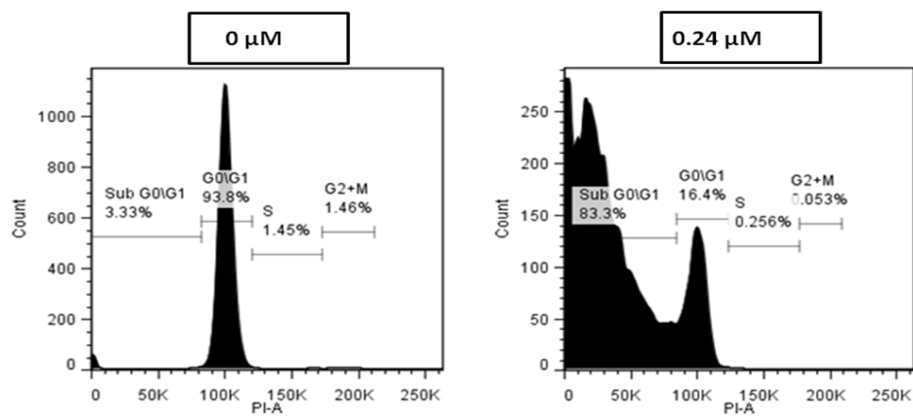


**Fig. 13.** Cell cycle analysis of A549 cells exposed to [Cu(TMCPMP-TS)(Phen)].

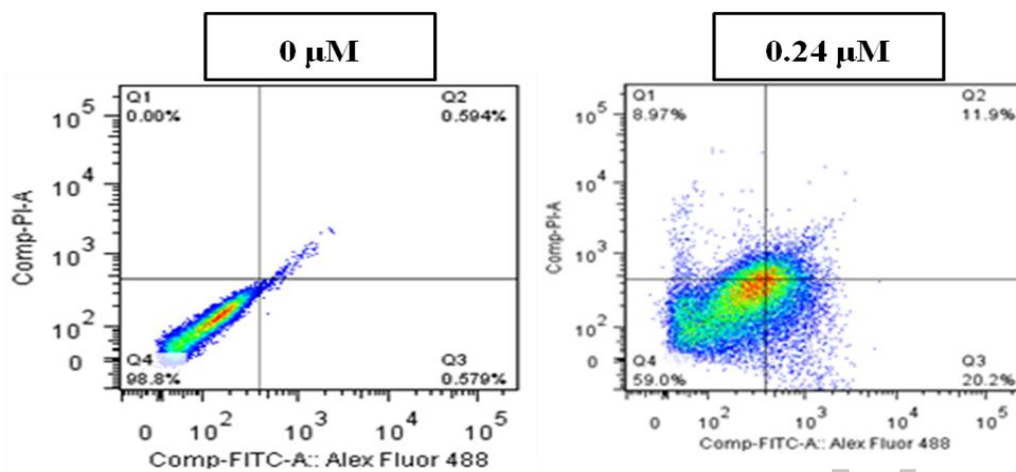
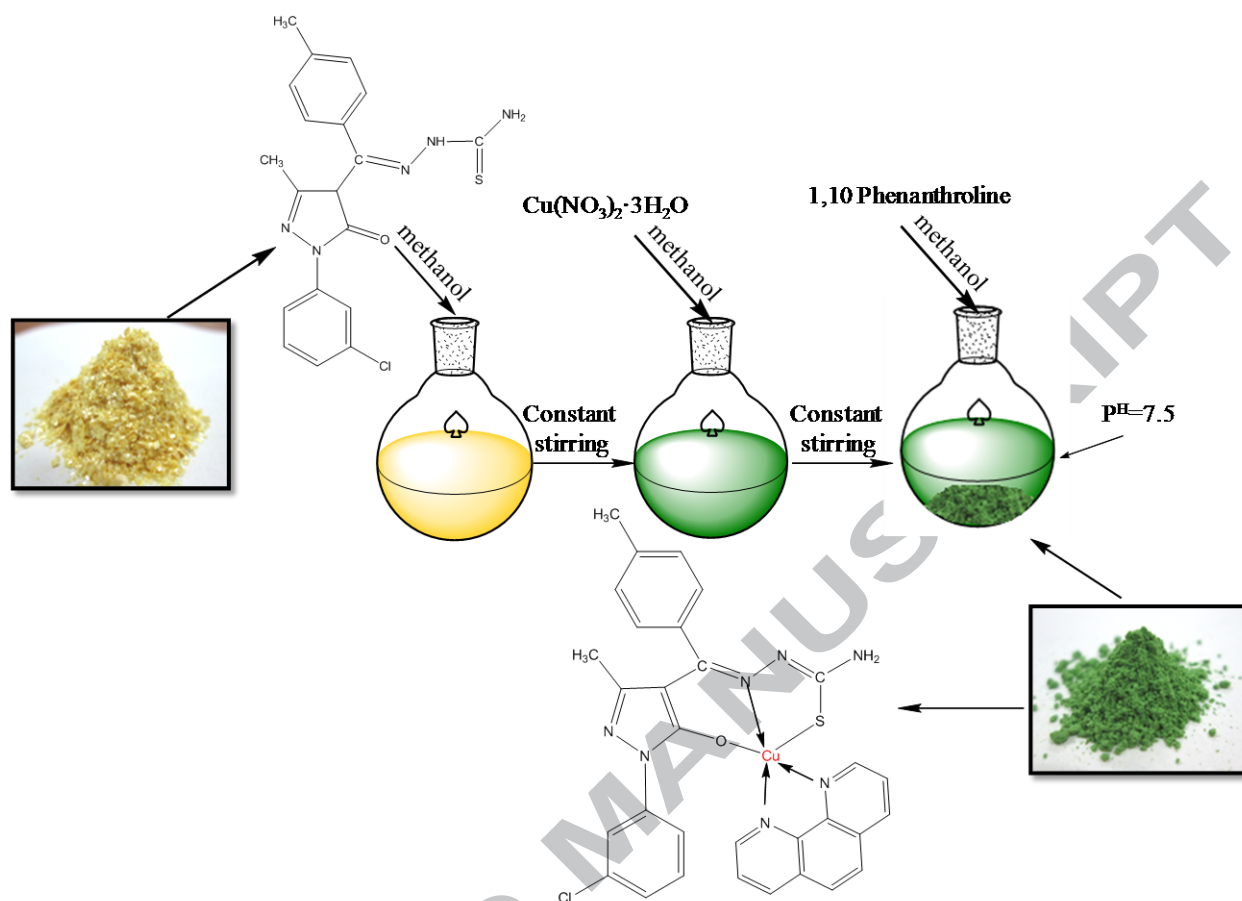


**Fig. 14.** Annexin V-Alexa fluoro 488/PI staining of A549 cells exposed to [Cu(TMCPMP-TS)(Phen)].



Scheme 1. Synthesis of the title complex

Table 1. Crystallographic data for the complex

| Compound                                  | [Cu(TMCPMP-TS)(Phen)]   |
|---|---|
| Chemical formula                          | C <sub>31</sub> H <sub>24</sub> ClCuN <sub>7</sub> OS, C <sub>2</sub> H <sub>6</sub> OS |
| Formula weight                            | 719.54  |
| Crystal description                       | Dark green block  |
| a (Å)                                     | 9.5066(4)   |
| b (Å)                                     | 11.8229(5)  |
| c (Å)                                     | 14.9547(5)  |
| α (°)                                     | 78.535(3)   |
| β (°)                                     | 79.135(3)   |
| γ (°)                                     | 83.427(3)   |
| Z   | 2   |
| V (Å <sup>3</sup> )                       | 1612.59(11)   |
| Reflection collected/unique               | 95559/6331  |
| R(int)                                    | 0.1094  |
| Number of parameters                      | 449   |
| Crystal system, Space group               | Triclinic, P-1  |
| Limiting indices                          | -13 ≤ h ≤ 13, -14 ≤ k ≤ 14, -15 ≤ l ≤ 15  |
| Crystal size                              | 0.3 x 0.2 x 0.2 mm  |
| ρ <sub>calcd.</sub> (g cm <sup>-3</sup> ) | 1.482   |
| Abs coeff, μ (cm <sup>-1</sup> )          | 0.933   |
| F(000)                                    | 742   |
| Temp (°C)                                 | 23  |
| GOF on F <sup>2</sup>                     | 1.065   |
| RI /wR2([I] > 2σ(I))                      | 0.0588/0.1238   |
| RI /wR2(all data)                         | 0.0905/0.1388   |

Table 2. Important bond lengths and bond angles

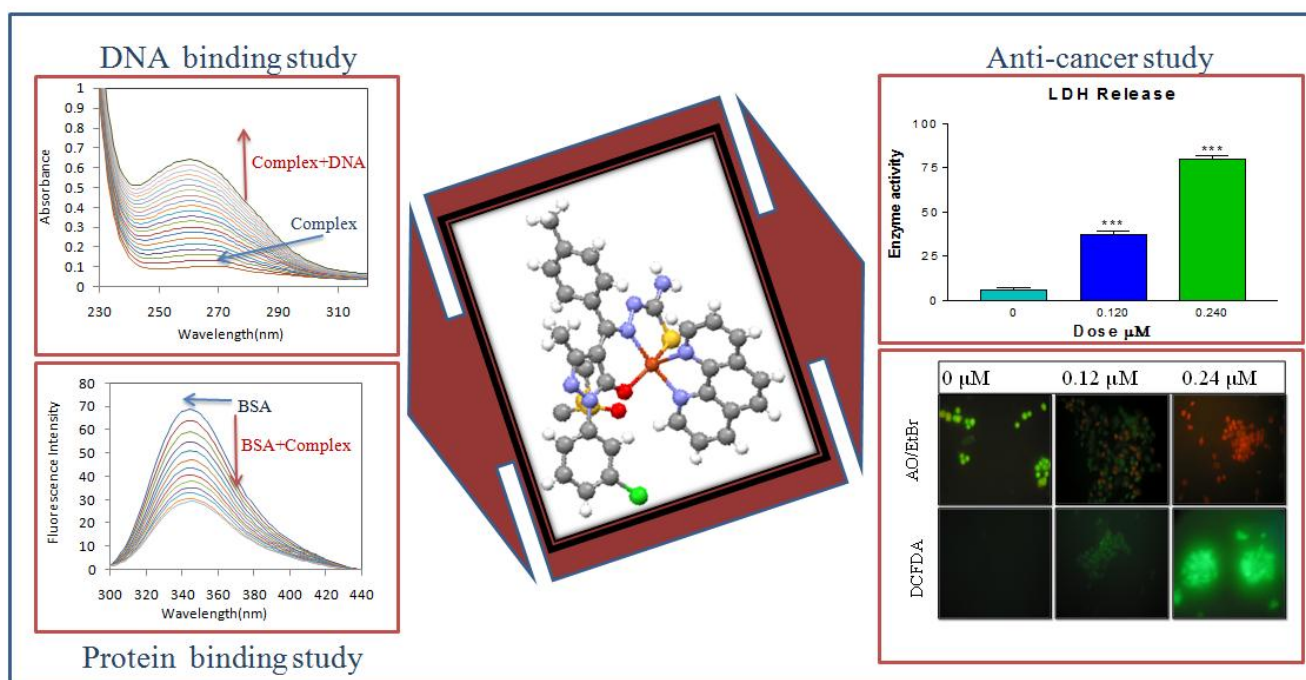
| Bond distances (Å)<br>with esd's in parentheses |            | Bond angles (Å)<br>with esd's in parentheses |            |
|---|------------|--|------------|
| Cu1 O1  | 1.932(3)   | O1 Cu1 N21                                   | 94.86(12)  |
| Cu1 N21   | 1.972(3)   | O1 Cu1 N26                                   | 88.35(12)  |
| Cu1 N26   | 2.033(3)   | N21 Cu1 N26                                  | 172.21(14) |
| Cu1 N37   | 2.261(4)   | O1 Cu1 N37                                   | 110.79(13) |
| Cu1 S25   | 2.2624(11) | N21 Cu1 N37                                  | 94.42(13)  |
| S25 C23   | 1.739(4)   | N26 Cu1 N37                                  | 77.80(13)  |
| O1 C5   | 1.279(4)   | O1 Cu1 S25                                   | 152.38(10) |
| N21 C13   | 1.320(5)   | N21 Cu1 S25                                  | 86.04(9)   |
| N21 N22   | 1.408(4)   | N26 Cu1 S25                                  | 94.40(10)  |
| N22 C23   | 1.309(5)   | N37 Cu1 S25                                  | 96.61(9)   |
| N24 C23   | 1.350(5)   | C23 S25 Cu1                                  | 93.63(13)  |
| N26 C27   | 1.311(5)   | C5 O1 Cu1                                    | 118.4(2)   |
| N26 C39   | 1.362(5)   | C13 N21 Cu1                                  | 125.0(3)   |
| N37 C36   | 1.323(5)   | N22 N21 Cu1                                  | 119.2(2)   |
| N37 C38   | 1.353(5)   | C27 N26 Cu1                                  | 126.5(3)   |
| N1 C5   | 1.378(5)   | C39 N26 Cu1                                  | 115.4(3)   |
| N1 N2   | 1.389(4)   | C36 N37 Cu1                                  | 131.6(3)   |
| N1 C6   | 1.417(5)   | C38 N37 Cu1                                  | 108.3(3)   |

Table 3. Geometry of the N-H...N hydrogen bonds

| D-H...A                         | D-H (Å) | D...A (Å) | H...A (Å) | D-H...A (°) |
|---------------------------------|---------|-----------|-----------|-------------|
| N24-H24A...N22 <sup>i</sup>     | 0.86    | 3.187     | 2.39      | 155         |
| Symmetry code: (i) -x, 2-y, 1-z |         |           |           |             |

Table 4. Changes observed in the bond distances on complexation

| Bond distance | Ligand   | Complex  | Effect   |
|---------------|----------|----------|----------|
| N21-N22       | 1.366(3) | 1.408(4) | Increase |
| C3-O3         | 1.253(2) | 1.279(4) | Increase |
| N22-C23       | 1.363(3) | 1.309(5) | Decrease |
| S25-C23       | 1.682(3) | 1.739(4) | Increase |
| C4-C13        | 1.481(3) | 1.422(5) | Decrease |
| C13-N21       | 1.286(3) | 1.320(5) | Increase |
| C23-N24       | 1.307(3) | 1.350(5) | Increase |



New synthesis of a new ternary complex [Cu(TMCPMP-TS)(Phen)] with crystal structure has been reported. The DNA binding, protein binding and anti-cancer studies of the complex has been studied.

The synthesis of a new ternary complex [Cu(TMCPMP-TS)(Phen)], with its crystal structure, has been reported. DNA binding, protein binding and anti-cancer studies of the complex has been carried out.

ACCEPTED MANUSCRIPT